Small-Angle X-ray Scattering Investigations of Ionomers with Variable-Length Side Chains

Robert B. Moore,[†] Diomar Bittencourt,[‡,§] Mario Gauthier,[†,∥] Claudine E. Williams,[*,‡] and Adi Eisenberg[*,†]

Department of Chemistry, McGill University, 801 Sherbrooke Street West, Montreal, Quebec, Canada H3A 2K6, and LURE (Laboratoire pour l'Utilisation du Rayonnement Electromagnétique), CNRS-CEA-MEN, Université Paris-Sud, 91405 Orsay, France

Received December 18, 1989; Revised Manuscript Received August 15, 1990

ABSTRACT: Small-angle X-ray scattering was used to investigate the morphology of random, styrene-based ionomers that have ionic groups placed at the ends of variable-length side chains. The SAXS peaks were interpreted as arising from interparticle interferences, and the changes in peak position with increasing side-chain length were attributed to increasing distances between the scattering centers. The decrease in the width of the SAXS peaks with increasing side-chain length was attributed to an increased organization of the ionic domains for the long side-chain ionomers. The Bragg spacing was found to increase linearly both with increasing side-chain length and with increasing average separation distance between the ionic groups. Furthermore, the radii of the ionic aggregates were found to be independent of the ionic content and limited in size by the proximity of the bulky polystyrene backbone. Since previous SAXS data from copolymers of polystyrene with cesium methacrylate are in excellent agreement with the morphological trends observed in this study, it is suggested that a morphological continuity exists for styrene ionomers that have their ionic groups placed very close to the backbone of ionomers with large separations between their ionic groups. By extension, the morphological continuity is suggested to also include the halato telechelics.

Introduction

During the past 20 years, the goal of an extensive number of investigations has been to understand and describe the complex microstructure of ionomers.[1-8] Even though great amounts of information concerning both the morphological characteristics and physical properties of ionomers are now available,[9-11] a controversy remains about the organization of the ionic groups in these materials. From small-angle X-ray scattering (SAXS) and neutron scattering (SANS) experiments,[12-22] the ion pairs of most ionomers have been shown to aggregate into domains of high ion content, which are surrounded by domains of low ion content. The precise structure and distribution of these ionic domains, however, is still under investigation.

Morphological models proposed for the microstructure of random ionomers typically treat the SAXS maximum (termed the "ionic peak") as arising from either interparticle or intraparticle interferences. The interparticle scattering models[13,19] have been used to describe the separation between the ionic aggregates, while the intraparticle scattering models[14,16] have been used to describe the internal structure of the aggregates. Nevertheless, the fact that ionomer morphology can be modeled from two completely different interpretations of the experimental data, and the fact that many assumptions or adjustable parameters are needed to fit the models to the SAXS data, suggests that much work remains to be done in this area.

The halato telechelic polymers are a family of "model" ionomers, which have received much attention in the last few years.[20,23-26] The ionic groups in these materials are located only at the ends of the polymer chains with a characteristic separation distance. The morphology of telechelics appears to be more straightforward than that of the typical random, polystyrene-based ionomers. SAXS investigations of dicarboxylatopolybutadiene telechelics (M_n = 4600) have shown that the ionic groups aggregate into multiplets (radius of ca. 9 Å for the alkaline-earth series) distributed in the organic matrix with a liquidlike order.[20,26] For monodisperse polyisoprene telechelics of different molecular weights, the average distance between the multiplets increases with the root-mean-square end-to-end distance between the ionic groups on the polymer. Provided this distance is well-defined, there is almost complete microphase separation between the organic and ionic moieties and the interface between them is sharp. The overall structure seems to be determined mainly by geometrical and space-filling arguments and depends very much on the configuration, size, and flexibility of the polymeric chain. Furthermore, these structural investigations[20,26] indicate that the morphology of telechelics cannot be described by an intraparticle, core–shell type model.[14,16]

In this investigation, we are interested in the morphology of random, styrene-based ionomers that have ionic groups placed at varying distances from the backbone.[27,28] Previous dynamic mechanical studies of these ionomers have shown an unsystematic dependence of ionic cross-linking efficiency on the side-chain length.[28] From these results, it was concluded that the unsystematic behavior could be attributed either to the proximity of the ionic groups to the bulky styrene backbone and/or solvating oxygen atoms or to the effects of side-chain length on backbone immobilization. An alternative explanation, however, may be that a morphological discontinuity exists as the distance between the ionic groups and the backbone increases. Therefore, a morphological investigation of these new materials is needed to understand more fully the link between ionomer morphology and their mechanical properties.

Since the morphology of the telechelics is governed by the separation between their ionic groups, we are also interested in comparing the effects of side-chain length on random ionomer morphology to the morphological

* To whom correspondence should be addressed.
† McGill University.
‡ Université Paris-Sud.
§ Permanent address: Instituto de Fisica, University of Sao Paulo, Sao Paulo CP20516, CEP 01498 Brazil.
∥ Present address: Institut für Makromolekulare Chemie, Universität Freiburg, D-7800 Freiburg, Federal Republic of Germany.

0024-9297/91/2224-1376$02.50/0

Chart I

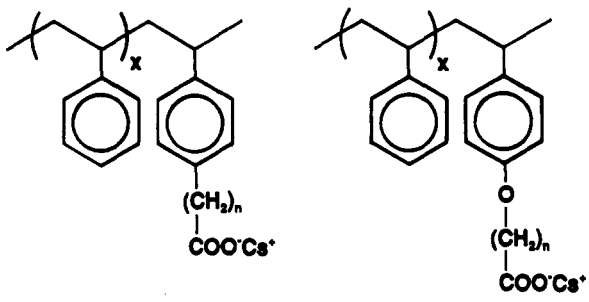

x = 8, 12
n = 1, 5, 10

Structure I

x = 7, 12
n = 1, 4, 10

Structure II

behavior of the telechelics. For the ionomers with very long side chains, the ionic groups are placed at the end of long hydrocarbon chains, and, thus, the packing of these ionic groups into multiplets is expected to be similar to the ionic aggregation found in the telechelics. In addition, by systematically varying the distance between the ionic groups and the polymer backbone, it is now possible to compare the process of ionic aggregation observed in typical, random ionomers such as poly(styrene-*co*-cesium methacrylate) to that of the telechelics. The results of these investigations are presented here.

Experimental Section

Materials. The synthesis of styrene ionomer precursors with *para*-methyl alkanoate side chains of variable length from 2 to 11 carbon atoms was described in a previous paper.[27] These materials were prepared either by direct attachment of the terminally carboxylated alkyl chains to the para position of the styrene rings (i.e., the alkyl derivatives, structure I; see Chart I) or through alkyl aryl ether linkages (i.e., the ether derivatives, structure II). The precursors used in this study were poly[styrene-*co*-4-(carbomethoxymethyl)styrene] (structure I, n = 1, termed C_2 alkyl), poly[styrene-*co*-4-(5-carbomethoxypentyl)styrene] (I, n = 5, termed C_6 alkyl), poly[styrene-*co*-4-(10-carbomethoxydecyl)styrene] (I, n = 10, termed C_{11} alkyl), poly[styrene-*co*-4-[(carbomethoxymethyl)oxy]styrene] (structure II, n = 1, termed C_2 ether), poly[styrene-*co*-4-[4-(carbomethoxybutyl)-1-oxy]styrene (II, n = 4, termed C_5 ether), and poly[styrene-*co*-4-[10-(carbomethoxydecyl)-1-oxy]styrene] (II, n = 10, termed C_{11} ether). The molecular weights, M_w (determined by gel permeation chromatography), of the alkyl and ether precursors were ca. 1.5×10^5 and 3×10^5, respectively.

The precursors were completely hydrolyzed by refluxing (under nitrogen) with excess sulfuric acid in a 90:10 tetraydrofuran/water solution for 3–5 days. Complete hydrolysis was confirmed by NMR spectroscopy. After washing and multiple precipitations in methanol, the carboxylic acid content was determined by titrating accurately weighed samples of the hydrolyzed polymers with a standard 0.05 N methanolic NaOH solution. The average acid content for the alkyl and ether derivatives was ca. 11% and 14% (per mole of styrene units), respectively.

Ionomeric forms of the esterified precursors were prepared by quantitatively hydrolyzing the polymers with CsOH. Typically, an accurately weighed precursor sample (ca. 1 g) was dissolved in 100 mL of 80:20 benzene/methanol solvent followed by the addition of 2 mL of water. Depending on the desired ionization level, a calculated amount of standard methanolic CsOH solution was added, and the polymer solution was then refluxed under nitrogen for 3–5 days. The ionized polymer was recovered by precipitation of the concentrated polymer solutions in methanol. Ionomers with two ion contents were prepared from both the alkyl- and ether-derivatized precursors. The 7.5 mol % alkyl series was prepared by hydrolyzing a fraction of the ester groups, and the 11 mol % series was prepared by complete hydrolysis. Similarly, the 7.5 mol % ether series was prepared by partial hydrolysis; however, the maximum ion content for the ether series was 14 mol %. The extent of ionization was confirmed by NMR analysis of the hydrolyzed polymers.[27]

Prior to molding, the precipitated ionomers were dried for 24 h at 60 °C in a vacuum oven. The SAXS samples were compression molded from approximately 0.1 g of the dried polymers at 30 °C above their respective cluster glass transition temperatures, $T_{g,c}$.[28] The heater was then turned off, and a pressure of ca. 28 MPa was maintained while the samples slowly cooled to room temperature. The samples were all ca. 1 mm thick and were stored in a desiccator until used for the SAXS analysis.

SAXS Instrumentation. The small-angle X-ray scattering experiments were conducted at the D22 station of the LURE-DCI synchrotron radiation source (Orsay, France). The fixed-exit, double-crystal monochromator[29] was tuned to provide a beam of 8.5-keV X-rays (λ = 1.46 Å). The size of the beam at the sample was about 1 mm^2. Two beam deflectors and NaI scintillator detectors were positioned before and after the sample chamber to constantly monitor the input X-ray intensity and sample absorption. The scattered X-rays were detected with a Xe–CO_2 gas-filled, one-dimensional, position-sensitive detector having a resolution of 152 μm.

The sample-to-detector distance was 460 mm. This distance allowed SAXS data to be obtained in the q-range from 0.006 to 0.42 Å^{-1} where $q = 4\pi \sin(\theta/\lambda)$, θ is half the scattering angle and λ is the X-ray wavelength. The SAXS data are plotted as the relative intensity versus q after correction for parasitic scattering and sample absorption. Furthermore, a background (assumed constant as a function of angle) was evaluated from a plot of $I(q)$ q^4 versus q^4 and subtracted from the scattering curve prior to data analysis. All samples were normalized to a thickness of 1 mm.

SAXS Data Analysis. For the ionomers studied here, the SAXS intensity profiles are treated as arising from a system of isolated particles (i.e., ionic aggregates in a polystyrene matrix), which occupy a negligible volume fraction of the total sample. Furthermore, the particles are assumed to have well-defined interfaces and a constant electron density. With use of standard scattering theories,[30,31] characteristic lengths pertaining to the morphology of the samples were obtained by combining the asymptotic form of the scattered intensity and the scattering invariant, Q, such that

$$\frac{\lim_{q\to\infty} I(q)\, q^4}{\int_0^\infty I(q)\, q^2\, dq} = \frac{K_P}{Q} = \frac{S}{\pi V} \tag{1}$$

where K_P is the Porod constant and S/V is the specific interfacial area. Equation 1 does not require absolute intensity measurements and provides a direct determination of the surface/volume ratio of the scattering particles. Assuming a spherical shape of the ionic aggregates, the S/V ratio may be used to calculate an approximate radius, R_a, of the ionic aggregates.

The number of ion pairs per aggregate, n_i, was estimated by dividing the aggregate volume (eq 1) by the molecular volume of model ionic compounds. For example, cesium formate ($HCOO^-Cs^+$) has a MW of 172.9 and a density of 1.017 g/cm^3, which yields a molecular volume of 281 Å^3. It should be noted that this method of calculating n_i is very dependent on the molecular parameters (e.g., the density) of the model ionic compound and should only be used as an estimate.

Simple space-filling calculations were also used to calculate n_i. These calculations are based on the assumptions that the SAXS peak is related to a characteristic center-to-center distance between ionic aggregates, and all of the ion pairs are in aggregates. The Bragg spacings were obtained from the peak maxima ($d_{Bragg} = 2\pi/q_{max}$) for each of the ionomer samples and related to n_i by

$$n_i = \frac{\rho N_A (d_{Bragg})^3}{EW} \tag{2}$$

where ρ is the polymer density (g/Å^3), N_A is Avagadro's number, and EW is the ionomer equivalent weight (g/mol) Since it is likely that a fraction of the ion pairs in random ionomers exist

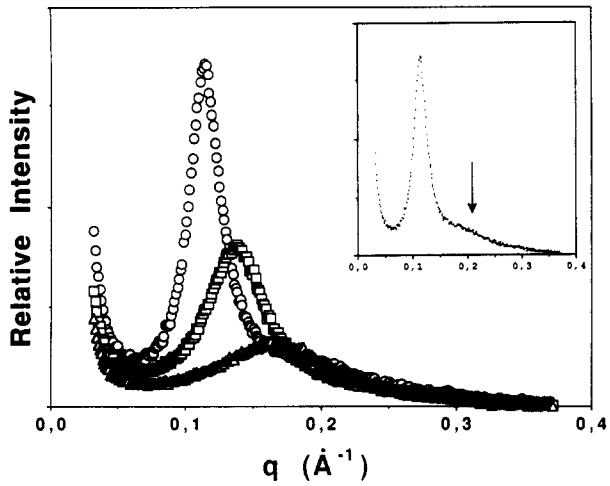

Figure 1. SAXS data for the partially hydrolyzed, alkyl ionomers. (○) C_{11} alkyl, (□) C_6 alkyl, and (△) C_2 alkyl. All samples were dry and converted to the Cs^+ form. The inset shows the SAXS profile for the partially hydrolyzed C_{11} alkyl ionomer. The arrow indicates the position of the second-order shoulder.

Table I
SAXS Data for the Alkyl Ionomers

sample	L_{sc},[a] Å	d_{Bragg}, Å	$\Delta q/q$[b]	R_a, Å
C_2 alkyl 7.5%	6.6	38.1	0.44	5.5
C_6 alkyl 7.5%	11.5	46.5	0.41	7.4
C_{11} alkyl 7.5%	17.8	55.6	0.27	10.9
C_2 alkyl 11%	6.6	34.1	0.38	5.6
C_6 alkyl 11%	11.5	40.5	0.32	7.4
C_{11} alkyl 11%	17.8	48.7	0.30	10.4

[a] Calculated from tabulated bond lengths and angles for extended chains. [b] The peak width at half-maximum divided by the peak position.

as lone ion pairs in the matrix,[19] these space-filling calculations should be considered as yielding an upper limit for n_i.

Results

Figure 1 shows a comparison of the SAXS intensity profiles for the C_2 alkyl, C_6 alkyl, and C_{11} alkyl ionomers, which contain 7.5 mol % of cesium carboxylate groups. Clearly, these three samples show typical ionic cluster peaks in the q-range of 0.1–0.2 $Å^{-1}$. Furthermore, the width and position of the SAXS peaks are observed to vary with the side-chain length. All of the other alkyl and ether ionomer samples have a similar behavior that is characteristic of systems where aggregation of the ionic groups has taken place. This confirms the results of previous dynamical mechanical studies,[28] which have shown that the mechanical properties of these materials are similar to the mechanical properties observed in other clustered, styrene-based ionomers. The presence of a second high-temperature peak in the loss tangent curves and the existence of SAXS "ionic" peaks for these ionomers are strong evidence that the ionic groups aggregate into phase-separated domains.

Tables I and II list the calculated, extended side-chain lengths, L_{sc}, the Bragg spacings, d_{Bragg}, quantitative measured of the SAXS peak widths $\Delta q/q$, and the radii of the ionic aggregates, R_a, for the alkyl and ether ionomers, respectively. These data show that the morphological parameters obtained from the SAXS intensity profiles are strongly influenced by the length of the ionic side chains. Inspection of the d_{Bragg} and $\Delta q/q$ data within the four distinct families (i.e., alkyl or ether, partially or completely hydrolyzed) shows that, for each family, the SAXS peaks shift to larger Bragg spacings (i.e., lower q_{max} values) and become significantly narrower (i.e., lower $\Delta q/q$ values) with an increase in the side-chain length. In addition, note that these data also show that the extent of hydrolysis and the mode of side-chain attachment in these polymers have little influence on this morphological trend.

Table II
SAXS Data for the Ether Ionomers

sample	L_{sc},[a] Å	d_{Bragg}, Å	$\Delta q/q$[b]	R_a, Å
C_2 ether 7.5%	8.0	40.0	0.51	6.0
C_5 ether 7.5%	11.5	48.0	0.46	7.2
C_{11} ether 7.5%	18.7	56.6	0.41	9.7
C_2 ether 14%	8.0	35.5	0.45	6.7
C_5 ether 14%	11.5	41.9	0.43	7.7
C_{11} ether 14%	18.7	51.1	0.27	10.4

[a] Calculated from tabulated bond lengths and angles for extended chains. [b] The peak width at half-maximum divided by the peak position.

Table III
Number of Ion Pairs per Aggregate for the Alkyl and Ether Ionomers

sample	$n_{i,f}$[a]	$n_{i,o}$[b]	$n_{i,s}$[c]	$\Delta\% n_i$
C_2 alkyl 7.5%	2.5	7.8	21	88
C_6 alkyl 7.5%	6.1	19	37	83
C_{11} alkyl 7.5%	20	61	60	67
C_2 alkyl 11%	2.7	8.2	20	86
C_6 alkyl 11%	5.9	18	33	82
C_{11} alkyl 11%	17	52	55	69
C_2 ether 7.5%	3.3	10	24	86
C_5 ether 7.5%	5.7	18	40	86
C_{11} ether 7.5%	14	42	63	78
C_2 ether 14%	4.5	14	28	84
C_5 ether 14%	6.8	21	44	85
C_{11} ether 14%	17	52	74	78

[a] Cesium formate as the model ionic compound: MW = 172.9; d = 1.017. [b] Cesium oxalate as the model ionic compound: MW = 353.8; d = 3.28. [c] Calculated from simple space-filling arguments (eq 2).

The most distinct change in peak width occurs when the side chains are lengthened from C_5 or C_6 to C_{11}. The inset of Figure 1 shows the SAXS intensity profile of the 7.5 mol % C_{11} alkyl ionomer. The arrow at $2q_{max}$ indicates the position of a second-order shoulder, which is similar in appearance to the shoulders observed in the scattering curves of monodisperse halato telechelic ionomers.[20] This shoulder indicates that the C_{11} ionomers are significantly more organized than the shorter side-chain ionomers. To the authors' knowledge, such second-order shoulders have never before been reported in polystyrene-based random ionomers.

Comparison of Table I with Table II shows that the Bragg spacings and radii of the ionic aggregates for the alkyl ionomers are identical (within experimental error) to those of the ether ionomers. Both d_{Bragg} and R_a increase dramatically with increasing L_{sc}. For a given side-chain length, the Bragg spacings for the partially hydrolyzed ionomers are larger than those for the completely hydrolyzed ionomers. This phenomenon of decreasing d_{Bragg} with increasing ion content has been documented for other random ionomers.[10,32] While d_{Bragg} is dependent on the ion content, it is important to note that R_a is independent of both the ion content and the mode of attachment of the side chains to the polystyrene backbone.

From the volume of the ion pairs (as estimated from the densities of model ionic compounds), the R_a may be used to calculate the number of ion pairs per aggregate, n_i. For each of the ionomer samples, Table III lists $n_{i,f}$ and $n_{i,o}$ calculated by using cesium formate (MW = 172.9; d = 1.02 g/mL) and cesium oxalate (MW = 353.8; d = 3.28) as

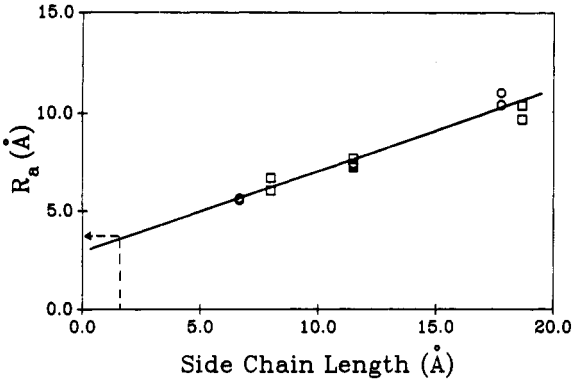

Figure 2. Plot of the aggregate radius, R_a, versus the side-chain length, L_{sc}, for the alkyl (filled symbols) and ether (open symbols) ionomers. The ○ and □ symbols refer to the partially and completely hydrolyzed ionomers, respectively. The dashed line is the extrapolation for poly(styrene-*co*-cesium methacrylate) ionomers (see text).

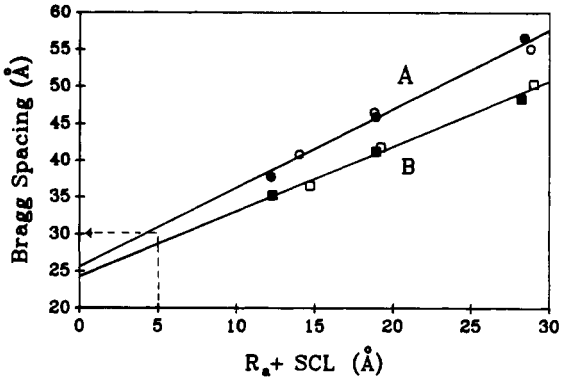

Figure 3. Plot of d_{Bragg} versus the sum of the aggregate radius and the side-chain length for the alkyl (○) and ether (□) ionomers. Lines A and B are the linear regression fits through the partially and completely hydrolyzed ionomers, respectively. The dashed line is the extrapolation for poly(styrene-*co*-cesium methacrylate) ionomers (see text).

model ionic compounds, respectively. It should be noted that n_i is strongly dependent on the molecular parameters of the model ionic compounds. For comparison, Table III also lists the $n_{i,s}$ obtained from simple space-filling calculations (eq 2) and the percent difference, $\Delta\% n_i$, between $n_{i,f}$ and $n_{i,s}$. These data clearly show that there is a dramatic increase in n_i as the distance between the polymer backbone and the ionic groups increases. Furthermore, as the side chain increases, $\Delta\% n_i$ decreases.

Figure 2 shows a plot of R_a versus L_{sc} for the variable-length side-chain ionomers. These data indicate that R_a increases linearly (slope = 0.41; correlation coefficient = 0.98) with increasing side-chain length. Since poly(styrene-*co*-cesium methacrylate) ionomers have the same ionic groups and polymeric backbone as the variable-length side-chain ionomers, the R_a for the very short side-chain, methacrylate ionomers may be estimated from the linear relationship observed in Figure 2. Thus, the L_{sc} for the methacrylate unit (ca. 1.5 Å) extrapolates to (dashed line) a R_a of ca. 3.5 Å.

Figure 3 shows a plot of d_{Bragg} versus the sum of R_a and the side-chain length, L_{sc}. Note that the quantity (R_a + L_{sc}) is the estimated distance from the center of the ionic aggregates to the polymer backbone. For the partially hydrolyzed ionomers (line A), d_{Bragg} increases linearly (slope = 1.1; correlation coefficient = 0.99) with increasing $R_a + L_{sc}$. An identical trend (line B) is observed with the completely hydrolyzed ionomers (slope = 0.9; correlation coefficient = 0.99). Due to the differences in ion content, the Bragg spacings of the completely hydrolyzed ionomers are lower with respect to the partially hydrolyzed ionomers. It is surprising, however, that the data for the 11 mol % alkyl and 14 mol % ether ionomers fall on the same line (line B). Possibly, at these high ionic contents, either the overall morphology becomes insensitive to the number of ions in the polymer or the differences fall within experimental error.

Since the radii of the ionic aggregates are determined from the S/V ratio (eq 1, which is independent of d_{Bragg}), the estimated R_a (from Figure 2), the known L_{sc}, and the linear relationships in Figure 3 may be used to predict a d_{Bragg} for the poly(styrene-*co*-cesium methacrylate) ionomers. The dashed line in Figure 3 indicates that these very short side-chain ionomers should yield Bragg spacings of ca. 30 Å. This extrapolated d_{Bragg} is in excellent agreement with previous SAXS results from 7.7 and 9.7 mol % poly(styrene-*co*-cesium methacrylate) ionomers.[32]

Discussion

Effect of Side-Chain Length on the SAXS Peak Width. If the ionomer SAXS peaks are attributed to scattering from particles arranged on a paracrystalline lattice and interpreted as scattering from a collection of particles with a distribution of repeat distances, then the peak maximum (i.e., d_{Bragg}) represents an estimate of the average repeat distance.[31] From this argument, the $\Delta q/q$ results suggest that the C_{11} ionomers contain ionic aggregates with a narrower distribution of scattering distances, and thus it seems reasonable to suggest that the C_{11} ionomers are better organized than the C_2 ionomers. This increased organization of the C_{11} ionomers is supported further by the appearance of a second-order shoulder observed in the scattering profile shown in Figure 1.

One explanation for the increased organization of the C_{11} ionomers may be attributed to the reduced steric constraints encountered by the ion pairs on the end of long side chains. As the distance between the ion pairs and the bulky polystyrene backbone increases, the ion pairs have a greater range of mobility and, thus, it is easier for the ion pairs to close-pack into aggregates of a more uniform size. For example, the ionic groups on the ends of long side chains that are located within a few monomer units of each other along the polymer backbone are able to reside in two difference ionic aggregates. This greater range of mobility lessens the dependence of the ionomer morphology on the randomness of the distance between ionic monomers along the polymer backbone. Conversely, when the ion pairs are located very close to the backbone, the decreased range of mobility and increased steric constraints encountered upon ionic aggregation cause a greater distribution in the number of ion pairs per aggregate and, thus, a greater distribution in the aggregate sizes.

A second explanation for a narrower distribution of scattering distances with increasing side-chain length may be due to the relative widths of the distribution of contour lengths (i.e., the separation distance between ionic groups along the side chains and backbone) for these polymers. Since the distance along the backbone that separates two side chains is random (i.e., average length if ca. 30 Å for the 7.5% ionomers), while the length of the side chains are monodisperse (i.e., $2L_{sc}$ is 14 and 36 Å for the C_2 and C_{11} ionomers, respectively), it follows that the short side-chain C_2 ionomers contain a statistically wider distribution of contour lengths than the C_{11} ionomers. Therefore, this wider contour length distribution yields a wider SAXS

peak for the short side-chain ionomers. While the contour length distribution and the effects of steric constraints on aggregate organization are independent explanations, it is reasonable to expect that both effects contribute significantly to the widths of the observed SAXS peaks.

Effect of the Side-Chain Length on the Radius of the Ionic Aggregates and the Bragg Spacing. Since R_a (Figure 2) is independent of both the ionic content and the mode of attachment (alkyl or ether linkage) of the side chains to the styrene rings, it is reasonable to conclude that the general morphological characteristics of these ionomers are primarily governed by the length of the side chains. This conclusion is further supported by the strong dependence of d_{Bragg} on the side-chain length (Tables I and II). For both the partially and completely hydrolyzed ionomers, plots of d_{Bragg} versus L_{sc} yield straight lines with slopes of ca. 1.45 and correlation coefficients of 0.995.

Many linear relationships are observed within the data set listed in Tables I and II. These relationships include Figure 2 and 3, d_{Bragg} versus L_{sc} and d_{Bragg} versus the contour length (slope = 0.64; correlation coefficient = 0.95). While all of these relationships appear to be quite linear, it should be noted that the molecular dimensions studied here are of a very limited range and any curvature in these plots may therefore be obscure. Nevertheless, since the morphology of the variable-length side-chain ionomers is observed to be a continuous function of the molecular dimensions within the polymer, these relationships are very important.

Other significant aspects of Figures 2 and 3 are the estimation of R_a and the accurate prediction of d_{Bragg} for poly(styrene-*co*-cesium methacrylate) ionomers. The morphology of these very short side-chain ionomers also must be dependent on the distance of the ionic groups from the bulky polystyrene backbone. Therefore, these data indicate that a morphological continuity exists between very short side-chain ionomers (i.e., polystyrene-*co*-cesium methacrylate) and the very long side-chain ionomers (i.e., C_{11} alkyl or ether ionomers).

The increase in d_{Bragg} with increasing side-chain length (Tables I and II) can be explained by considering the effect of side-chain length on the size of the ionic aggregates. This consideration involves the relative ability of the ion pairs to pack into organized ionic domains. When the ion pairs aggregate, the steric constraints encountered during close-packing limit the number of ion pairs incorporated into the aggregate.[1] If ionic groups are placed very close to the polymer backbone, then the proximity of the bulky backbone and phenyl rings allows for the close-packing of only a few ion pairs. Conversely, as the distance between the ion pairs and the bulky polystyrene backbone increases, the close packing of the low-volume hydrocarbon side chains allows for the incorporation of more ion pairs into the aggregates and thus the size of the aggregates increases. This phenomenon is clearly demonstrated in Figure 2. As the ionic groups are spaced further from the backbone, the size of the ionic aggregates increases.

The ability of steric constraints to limit the number of ion pairs per aggregate is shown in Table III. Simple space-filling calculations of the number of ion pairs per aggregate, $n_{i,s}$, and calculations based on the volume of the ionic aggregates (i.e., $n_{i,f}$ and $n_{i,o}$) show that the aggregates in the C_{11} ionomers contain many more ion pairs than the C_2 ionomers. It is important to note that the values in Table III are estimates. For example, a comparison of $n_{i,f}$ to $n_{i,o}$ shows the sensitivity of these values to the packing density of the model ionic compounds. Since $n_{i,s}$ is based on the assumption that all of the ion pairs are in aggregates and $n_{i,f}$ for the C_2 ionomers seems too low for sufficient scattering contrast, we feel that $n_{i,s}$ and $n_{i,f}$ should be considered as the upper and lower limits, respectively.

Because it is unlikely that all of the ion pairs reside in aggregates,[19] the difference between the upper and lower limits may indicate a change in the relative number of lone ion pairs in the polymer matrix. The data in Table III show that $\Delta\% n_i$ decreases with increasing I_{sc}. Thus, it seems reasonable to conclude that the C_{11} ionomers have a fewer number of lone ion pairs in the polymer matrix relative to the C_2 ionomers. Due to the lack of absolute values for n_i, an estimate of the number of lone ion pairs in these ionomers is not feasible. However, this conclusion of a decreasing number of lone ion pairs with increasing L_{sc} is consistent with the increased organization of the long side-chain ionomers.

For very long side chains, ther steric constraints from the backbone are expected to be negligible in governing the size of the ionic aggregates. Assuming the aggregates maintain a constant shape, the maximum size of the aggregates is controlled only by the packing efficiency of the side chains, as has been found in the telechelics.[20,26] In a manner analogous to the formation of inverted micelles, the packing efficiency is dependent on the relative sizes of the ion pairs and the cross-sectional area of the side chains. Therefore, since the data in Figure 2 and Table III indicate that R_a and thus n_i are increasing with the side-chain length, it appears that ionic aggregation in these ionomers is still influenced by the steric constraints from the bulky polystyrene backbone.

Comparison of Random Ionomers to the Halato Telechelics. As mentioned in the Introduction, the end-to-end chain length between ionic groups and the distribution of this length have been shown to be relevant parameters in governing the morphology of halato telechelic "model" ionomers.[26] Although the variable-length side-chain ionomers are random copolymers, the separation distance between ionic groups along the polymer chain and the distribution of this distance also appear to be relevant morphological parameters. For example, the ionomers studied here yield Bragg spacings that are within 20% of their calculated center-to-center interaggregate distances ($2R_a$ + the average rms contour length).

In the telechelics, the MW range was wide and d_{Bragg} was found to vary linearly with $M^{0.45}$; this relationship is compatible with a coil conformation of the chains between the ionic end groups.[20,26] For the variable-length side-chain ionomers, d_{Bragg} also varies linearly with M^1, $M^{1/2}$, and $M^{1/3}$. These apparent linear relationships are most probably due to the very narrow MW range under investigation. As with the telechelics,[20] the intercepts of the $M^{1/2}$ relationships observed with these random ionomers are much closer to zero than those for the M^1 or $M^{1/3}$ relationships. Although the average, random-coil dimensions between the ionic groups are only slightly smaller than the extended chain dimensions, these data suggest that the polymer chains between the ionic groups adopt a random-coil conformation.

If L_{sc} was increased to lengths approaching those of the telechelics, then the ionic aggregates would reach their maximum size (as discussed above) and d_{Bragg} would only be a function of the rms end-to-end distance between the ionic groups. Thus, since the ion pairs at the end of long side chains are expected to pack into aggregates in a manner identical with the ionic aggregation in the telechelics, we believe that the morphological continuity indicated in Figure 3 extends from ionomers with very short side chains all the way to the telechelics.

Finally, the conclusion that the morphology of the telechelics cannot be described by an intraparticle type model[20,26] is of great importance to this investigation. From the morphological continuity argument, it seems reasonable to suggest that the SAXS peaks observed in these random ionomers are also of interparticle origin. Furthermore, it is important to note that these findings became an integral feature in the development of a new model for the morphology of random ionomers.[33]

Correlation between Ionomer Morphology and Dynamic Mechanical Behavior. An important aspect of Figures 2 and 3 is the comparison of the ether ionomers to the alkyl ionomers. Previous dynamic mechanical investigations of these ionomers showed that the mechanical properties of the ether ionomers were somewhat different from those of the alkyl ionomers.[28] These differences became more pronounced as the side-chain length decreased and were attributed to a diminished degree of ionic aggregation in the polymers that contained solvating oxygen atoms in the alkyl aryl ether linkages. From the SAXS data, however, the size and spatial arrangement of the ionic aggregates in both the alkyl and ether ionomers are identical. Therefore, it appears that the presence of solvating oxygen atoms does not affect the overall morphology of these materials.

As mentioned in the Introduction, the variable-length side-chain ionomers also show unsystematic mechanical properties as the length of the side chains increases. The SAXS data, however, indicate a very systematic variation in the morphology of these materials with increasing side-chain length. Therefore, we now attribute the unsystematic mechanical properties to backbone immobilization effects. As the side-chain length increases the immobilization due to the proximity of the ionic groups to the backbone decreases. In contrast, the backbone immobilization due to the size of the ionic aggregates increases with side-chain length. These two competing effects allow for high backbone immobilization (i.e., high apparent cross-linking efficiency) from either very short or very long side-chain lengths. Immobilization reaches a minimum at intermediate side-chain lengths. Thus, this argument explains why the long C_{11} side-chain ionomers and the poly(styrene-*co*-sodium methacrylate) ionomers demonstrate high apparent cross-linking efficiencies, while in the C_2 through C_6 ionomers, it is significantly lower.[28]

Conclusions

For both the alkyl and ether ionomers, the length of the side chain was found to influence the overall organization of the ionic aggregates. As the side-chain length increased, the ionic aggregates became larger and more organized, resulting in narrower SAXS peaks at lower q values. The narrow peaks and second-order shoulders observed for the C_{11} ionomers were attributed to scattering from a narrower distribution of interparticle distances as compared to the C_2 ionomers.

The d_{Bragg} was found to increase linearly with increasing side-chain and contour lengths. These apparent linear relationships were attributed to the very narrow range of MW between the ionic groups; however, the data clearly indicate that a morphological continuity exists from ionomers that have their ionic groups placed very close to the polymer backbone to ionomers with ionic groups located far from the backbone. In addition, the mode of attachment of the side chain to the polystyrene backbone (i.e., alkyl or ether linkage) was found to have no effect on the overall morphology of these ionomers.

For both the variable-length side-chain ionomers and halato telechelic ionomers, the end-to-end distance between the ionic groups and the distribution of this distance are relevant morphological parameters. Since the ionic groups at the end of long side chains are expected to pack into aggregates in a manner identical with that of the telechelics, a morphological continuity is suggested to extend from ionomers with the ionic groups placed very close to the backbone all the way to the telechelics. Furthermore, this morphological link between the random ionomers and the telechelics suggests that the SAXS "ionic" peaks in random ionomers originate from interparticle scattering.

Previous investigations of the alkyl and ether ionomers with variable-length side chains have shown unsystematic trends in their dynamic mechanical properties.[28] By contrast, the SAXS results presented in this investigation clearly show that changes in the length of the side chains cause very systematic variations in the morphological characteristics of these ionomers. This indicates that the observed trends in the mechanical properties are not due to unsystematic morphological changes. We relate the mechanical behavior of these polymers to backbone immobilization effects.

Acknowledgment. Support for this work was provided by the U.S. Army Research Office and NSERC (Canada). We gratefully acknowledge the travel support from the NATO collaborative Grant 0504/86. D.B. acknowledges the CNPq (Brazil) for financial support. We also acknowledge the reviewers of this manuscript for their helpful comments.

References and Notes

(1) Eisenberg, A. *Macromolecules* **1970**, *3*, 147.
(2) Holliday, L., Ed. *Ionic Polymers*; Applied Science Publishers: London, 1975.
(3) Eisenberg, A.; King, M. *Ion-Containing Polymers, Physical Properties and Structure*; Academic Press: New York, 1977.
(4) Eisenberg, A., Ed. *Ions in Polymers*; Advances in Chemistry Series 187; American Chemical Society: Washington, DC, 1980.
(5) Wilson, A. D., Prosser, H. J., Eds. *Developments in Ionic Polymers*—1; Applied Science Publishers: New York, 1983.
(6) Eisenberg, A., Bailey, F. E., Eds. *Coulombic Interactions in Macromolecular Systems*; ACS Symposium Series 302; American Chemical Society: Washington, DC, 1986.
(7) Pineri, M., Eisenberg, A., Eds. *Structure and Properties of Ionomers*; NATO Advanced Study Institute Series 198; D. Reidel Publishing Co.: Dordrecht, Holland, 1987.
(8) Mauritz, K. A. *J. Macromol. Sci., Rev. Macromol. Chem. Phys.* **1988**, *C28*, 65.
(9) MacKnight, W. J.; Earnest, T. R., Jr. *J. Polym. Sci., Macromol. Rev.* **1981**, *16*, 41.
(10) Fitzgerald, J. J.; Weiss, R. A. *J. Macromol. Sci., Rev. Macromol. Chem. Phys.* **1988**, *C28*, 99.
(11) Tant, M. R.; Wilkes, G. L. *J. Macromol. Sci., Rev. Macromol. Chem. Phys.* **1988**, *C28*, 1.
(12) Wilson, F. C.; Longworth, R.; Vaughan, D. J. *Polym. Prepr. (Am. Chem. Soc., Div. Polym. Chem.)* **1968**, *9*, 505.
(13) Marx, C. L.; Caulfield, D. F.; Cooper, S. L. *Macromolecules* **1973**, *6*, 344.
(14) MacKnight, W. J.; Taggart, W. P.; Stein, R. S. *J. Polym. Sci., Polym. Symp.* **1974**, *45*, 113.
(15) Roche, E. J.; Stein, R. S.; MacKnight, W. J. *J. Polym. Sci., Polym. Phys. Ed.* **1980**, *18*, 1035.
(16) Roche, E. J.; Stein, R. S.; Russell, T. P.; MacKnight, W. J. *J. Polym. Sci., Polym. Phys. Ed.* **1980**, *18*, 1497.
(17) Earnest, T. R.; Higgins, J. S.; Handlin, D. L.; MacKnight, W. J. *Macromolecules* **1981**, *14*, 192.
(18) Peiffer, D. G.; Weiss, R. A.; Lundberg, R. D. *J. Polym. Sci., Polym. Phys. Ed.* **1982**, *20*, 1503.
(19) Yarusso, D. J.; Cooper, S. L. *Macromolecules* **1983**, *16*, 1871.
(20) Williams, C. E.; Russell, T. P.; Jérôme, R.; Horrion, J. *Macromolecules* **1986**, *19*, 2877.
(21) Galambos, A. F.; Stockton, W. B.; Koberstein, J. T.; Sen, A.; Weiss, R. A.; Russell, T. P. *Macromolecules* **1987**, *20*, 3094.
(22) Register, R. A.; Sen, A.; Weiss, R. A.; Cooper, S. L. *Macromolecules* **1989**, *22*, 2224.
(23) Tant, M. R.; Song, J. H.; Wilkes, G. L.; Horrion, J.; Jérôme, R. *Polymer* **1986**, *27*, 1815.

(24) Horrion, J.; Jérôme, R.; Teyssié, Ph.; Marco, L.; Williams, C. E. *Polymer* **1988**, *29*, 1203.
(25) Register, R. A.; Foucart, M.; Jérôme, R.; Ding, Y. S.; Cooper, S. L. *Macromolecules* **1988**, *21*, 1009.
(26) Williams, C. E. In *Multiphase Macromolecular Systems*; Culbertson, W. M., Ed.; Plenum Press: New York, 1989.
(27) Gauthier, M.; Eisenberg, A. *J. Polym. Sci.: Part A: Polym. Chem.* **1990**, *28*, 1549.
(28) Gauthier, M.; Eisenberg, A. *Macromolecules* **1990**, *23*, 2066.
(29) Dubuisson, J. M.; Dauvergne, J. M.; Depautex, C.; Vachette, P.; Williams, C. E. *Nucl. Instr. Meth.* **1986**, *A246*, 636.
(30) Glatter, O.; Kratky, O. *Small Angle X-ray Scattering*; Academic Press: New York, 1982.
(31) Guinier, A.; Fournet, G. *Small-Angle Scattering of X-Rays*; John Wiley and Sons, Inc.: New York, 1955.
(32) Roche, E. J. Ph.D. Thesis, Polymer Science and Engineering Department, University of Massachusetts, 1978.
(33) Eisenberg, A.; Hird, B.; Moore, R. B. *Macromolecules* **1990**, *23*, 4098.